

1 **Supplementary information**

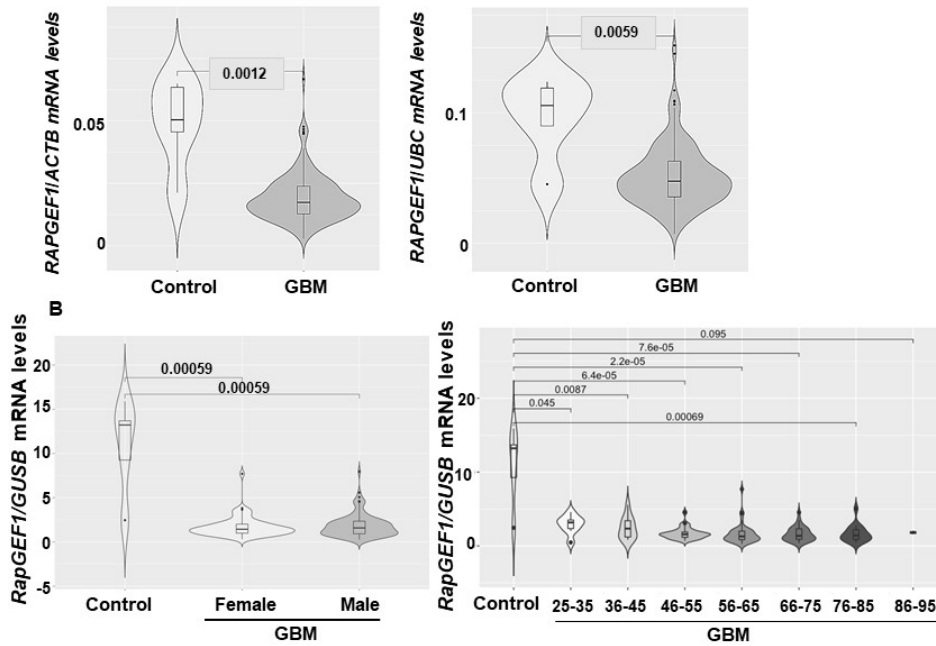
2

3 **Primers used for RT-qPCR analysis**

4 Primers used for: *TWIST1* f-CAAAGAAACAGGGCGTGGGG and r-  
5 CAGAGGTGTGAGGATGGTGCC; *ZEB2* f-AATGCACAGAGTGTGGCAAGGC and r-  
6 ATCTGGCGTTCCAGGGACTCAT; *GUSB* f-ATCACCGTCACCACCAGCGT and r-  
7 GTCCCATTCGCCACGACTTTG.

8

9 **Supplementary figures**



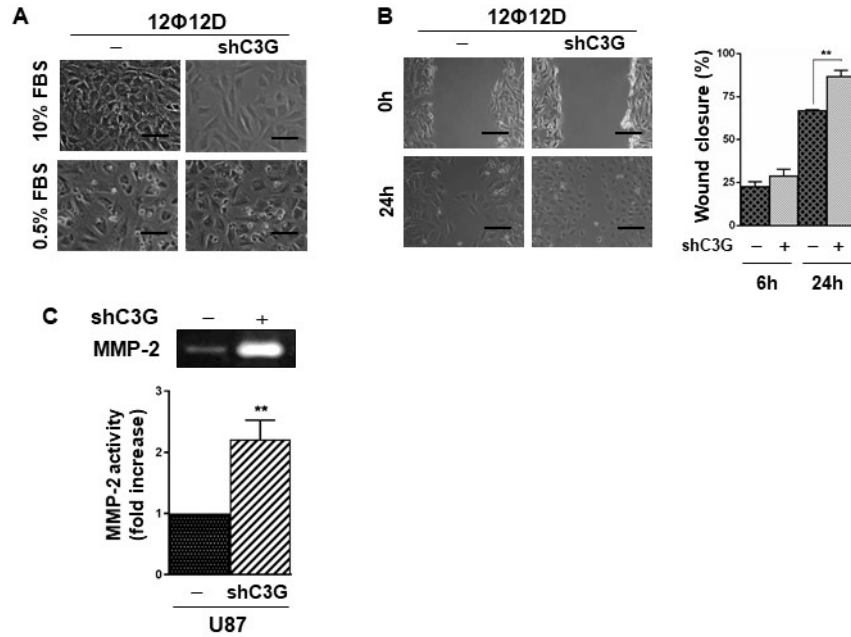
10

11 **Supplementary Figure 1—Analysis of C3G expression in glioblastoma patient samples. (A)**

12 RapGEF1 mRNA levels in glioblastoma patient samples normalized with different housekeeping

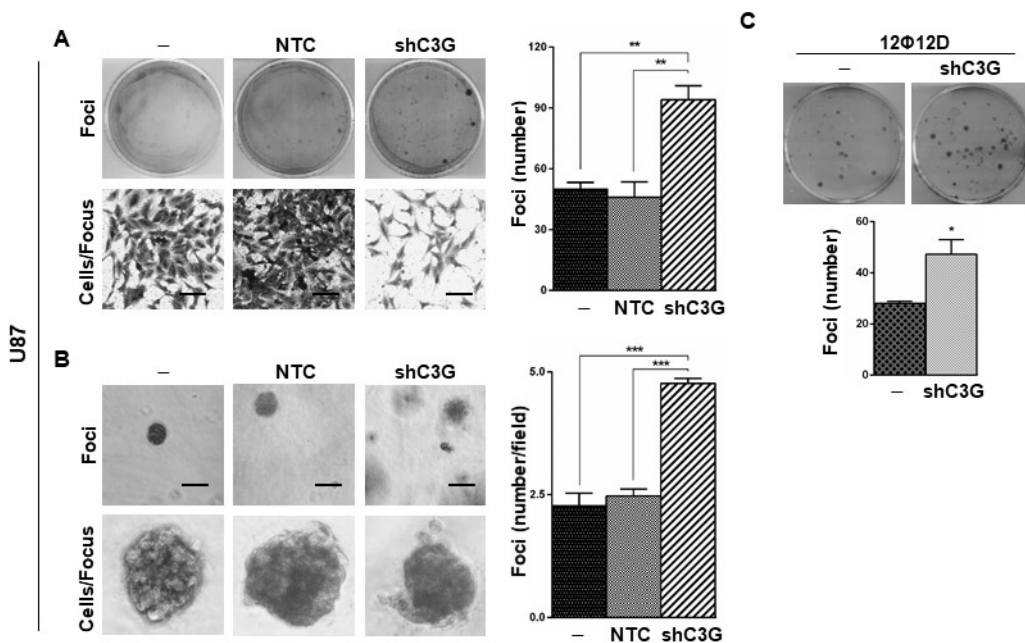
13 genes: left panel, *ACTB* ( $\beta$ -actin) and right panel, *UBC* (ubiquitin C). **(B)** *RAPGEF1* mRNA levels in

14 GBM patient samples grouped by sex (left panel) or age (right panel).



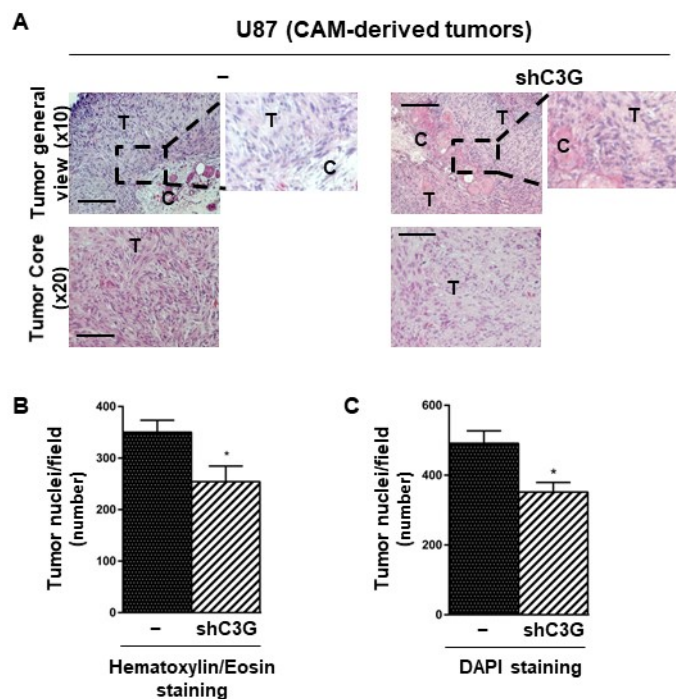
15

16 **Supplementary Figure 2—C3G down-regulation enhances migration of 12Φ12D glioblastoma**  
 17 **cells. Lack of effect of non-targeting shRNAs on invasive properties of GB U87 cells. (A)**  
 18 Representative phase contrast microscopy images of 12Φ12D cells morphology. Scale bars: 50  
 19 μm. **(B)** Wound healing assay in 12Φ12D cells. Left panel, representative phase contrast  
 20 microscopy images at 0h and 24h of migration; right panel, histogram represents the mean value  
 21 of wound closure percentage ± S.E.M. at 6 and 24h (n=3-4). \*\*p<0.01 C3G silenced cells versus  
 22 non-silenced. Scale bars: 100 μm. **(C)** Zymographic analysis of MMP2 activity of non-silenced  
 23 and C3G silenced U87 cells using culture medium from 24h serum-deprived cells that is  
 24 submitted to electrophoresis in 8% SDS-polyacrylamide-0.1% gelatin gels under non-reducing  
 25 conditions<sup>1</sup>. Upper panel, representative zymogram; lower panel, histogram showing the fold  
 26 increase of MMP-2 activity (mean value ± S.E.M., n=5), p<0.01, compared to non-silenced cells.



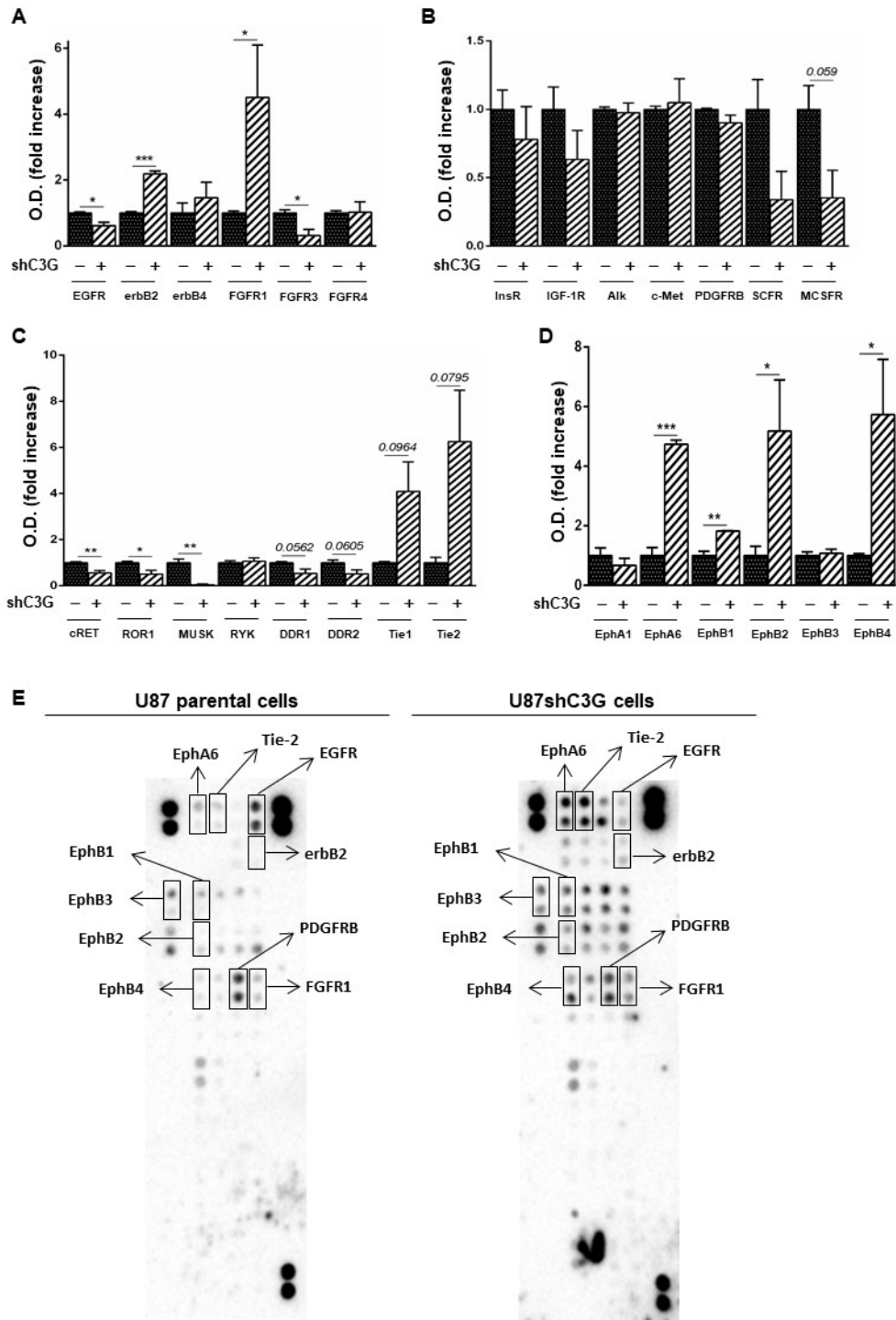
27

28 **Supplementary Figure 3–Non-targeting shRNAs does not interfere with tumorigenic**  
 29 **properties of glioblastoma cells. (A) and (B) Effect of non-targeting shRNAs (NTC) as compared**  
 30 **to parental and C3G silenced U87 cells. (A) Anchorage-dependent growth. Left panels,**  
 31 **representative images of foci macroscopic view (upper panel) and cells within an individual focus**  
 32 **(lower panel); right panel, histogram showing the mean value  $\pm$  S.E.M. of foci number (n=3).**  
 33 **Scale bars: 100  $\mu$ m. (B) Anchorage-independent growth. Left panel, representative images of foci**  
 34 **microscopic view (upper panel) and cell organization within an individual focus (lower**  
 35 **panel); right panel, histogram showing the mean value  $\pm$  S.E.M. of foci number (n=3). Scale bars:**  
 36 **100  $\mu$ m. (C) Effect of C3G silencing on anchorage-dependent growth of 12 $\Phi$ 12D cells. Upper**  
 37 **panel, representative images of foci macroscopic view; lower panel, histogram showing the**  
 38 **mean value  $\pm$  S.E.M. of foci number (n=3). \*p $\leq$ 0.05, \*\*p $\leq$ 0.01, \*\*\*p $\leq$ 0.001, compared as**  
 39 **indicated.**



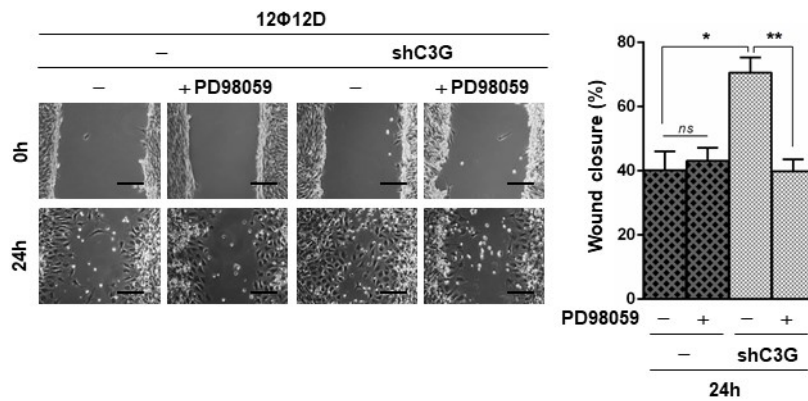
40

41 **Supplementary Figure 4–Analysis of the morphology and cell density of tumors generated by**  
 42 **parental and C3G-silenced U87 cells in CAM assays. (A) Hematoxylin/eosin staining of tumor**  
 43 **sections. Phase contrast microscopy images. Upper panel: left side, general view at 10x**  
 44 **magnification, where the tumor (T) and the CAM tissue (C) can be visualized; right side,**  
 45 **magnification of the rectangle area. Lower panel, view of tumor core at 20x magnification. Scale**  
 46 **bars: 100  $\mu$ m (upper panel) and Scale bars: 50  $\mu$ m (lower panel). (B and C) Histograms showing**  
 47 **the mean value  $\pm$  S.E.M. of the number of tumor cells or nuclei per field from CAM derived**  
 48 **tumors stained with hematoxylin/eosin (B) or with anti- $\alpha$ SMA (C) (n=3). \*p $\leq$ 0.05 compared as**  
 49 **to tumors derived from non-silenced cells.**



50

51 **Supplementary Figure 5—Effect of C3G silencing on phosphorylation of RTKs using an array. (A,**  
 52 **B, C and D)** Histograms represent the mean value  $\pm$  S.E.M. of the densitometric quantification  
 53 of the phosphorylation levels of RTKs in parental and C3G silenced U87 cells (n=2). **(E)**  
 54 Representative images of the membranes, where some RTK phosphorylation spots are  
 55 indicated. \* $p \leq 0.05$ , \*\* $p \leq 0.01$ , \*\*\* $p \leq 0.001$  compared as indicated.



56

57 **Supplementary Figure 6-ERKs inhibition prevents the increase in migration induced by C3G**  
 58 **silencing in 12Φ12D glioblastoma cells.** Wound healing assay in 12Φ12D cells maintained  
 59 untreated or treated with PD98059. Left panels, representative phase contrast microscopy  
 60 images at 0h and 24h of migration; right panel, histogram represents the mean value of wound  
 61 closure percentage ± S.E.M. at 24h (n=3-4). \*p≤0.05, \*\*p≤0.01, compared as indicated. Scale  
 62 bars: 100 μm.

63 **References**

- 64 1. Priego N, Arechederra M, Sequera C, Bragado P, Vazquez-Carballo A, Gutierrez-Uzquiza  
 65 A, *et al.* C3G knock-down enhances migration and invasion by increasing Rap1-  
 66 mediated p38alpha activation, while it impairs tumor growth through p38alpha-  
 67 independent mechanisms. *Oncotarget* 2016, **7**(29): 45060-45078.

68